Available online at www.sciencedirect.com
SCIENCE DIRECT®
ELSEVIER
Journal of Crystal Growth 287 (2006) 637–641
JOURNAL OF CRYSTAL GROWTH
www.elsevier.com/locate/jcrysgro

# In situ determination and control of AlGaInP composition during MOVPE growth

M. Zorn[a,*], J.-T. Zettler[b], A. Knauer[a], M. Weyers[a]

[a]Ferdinand-Braun-Institut für Höchstfrequenztechnik (FBH), Gustav-Kirchhoff-Str. 4, D-12489 Berlin, Germany
[b]LayTec GmbH, Helmholtzstr. 13-14, D-10587 Berlin, Germany

**Abstract**

The influence of composition changes in $(Al_xGa_{1-x})_{1-y}In_yP$ grown on GaAs in metal-organic vapour-phase epitaxy on the in situ measured optical signals reflectance anisotropy (RA) and normalized reflectance (NR) is studied. The aluminium composition $x$ (band gap) is changed from 0 to 1 while the indium composition $y$ (lattice matching) is adjusted about $\pm 0.03$ around the lattice matched value of $y = 0.48$. The optical signals were correlated to the composition which was determined by ex situ measurements. A strong influence of both compositions $x$ and $y$, respectively, is observed in the RA and the NR spectra and transients. The composition changes have an influence on the amplitude as well as on the energetic positions of the respective features in the RA spectra. A strong influence of the composition on the first amplitude of the UV Fabry–Perot interference in the time-resolved NR signal can be seen. Very thin layers, 12 nm, are sufficient for the in situ determination of the composition. The results are used for in situ composition calibration procedures.
© 2005 Published by Elsevier B.V.

*PACS:* 81.05.Ea; 81.15.Gh; 78.40.Fy; 78.66.Fd

*Keywords:* A1. In situ monitoring; A3. Metalorganic vapour-phase epitaxy; B2. Semiconducting AlGaInP

## 1. Introduction

AlGaInP lattice matched to GaAs is a key material in opto-electronic devices like light-emitting diodes (LED) [1], edge-emitting lasers (EEL) [2] and vertical-cavity surface-emitting lasers (VCSEL) [3] for the visible red wavelength range. Changing the aluminium content in $(Al_xGa_{1-x})_{0.52}In_{0.48}P$ from 0 to 1 shifts the emission wavelength in the range from about 650–550 nm before becoming an indirect material at about $x = 0.7$. Furthermore, $(Al_xGa_{1-x})_{0.52}In_{0.48}P$ with high $x$ values is the only possible barrier material in red EELs and VCSELs. A tight control of the aluminium composition (band gap) and indium content (lattice matching) is therefore highly desired during growth in metal-organic vapour-phase epitaxy (MOVPE).

In situ reflectance anisotropy spectroscopy (RAS) [4,5] and normalized reflectance (NR) measurements have proven their potential for the development of growth processes for opto-electronic device structures [6]. It has been shown that it is possible to control the composition in InGaAsP grown on InP in MOVPE in situ using a combination of RAS and NR measurements [7]. However, the situation in this material system is much more simple since this material consists of two group III and two group V components. For $(Al_xGa_{1-x})_{1-y}In_yP$ the situation is more challenging because of the three group III components used. Recently, Watatani et al. [8] demonstrated the possibility of correlating the in situ measured reflectance at 2.3 eV to the Al/Ga ratio in their AlGaInP layers. However, the In content for lattice-matched growth has not been measured in-situ yet.

In this work we first investigated the influence of composition changes in $(Al_xGa_{1-x})_{1-y}In_yP$ for both compositions $x$ and $y$ on the optical signals RAS and NR. Based on these results the possibility of in situ calibration procedures is discussed.

*Corresponding author. Tel.: +49 30 6392 2676; fax: +49 30 6392 2685.
*E-mail address:* martin.zorn@fbh-berlin.de (M. Zorn).

0022-0248/$ - see front matter © 2005 Published by Elsevier B.V.
doi:10.1016/j.jcrysgro.2005.10.120

## 2. Experimental procedure

The layer structures presented here were grown by MOVPE in a horizontal Aixtron 200/4 reactor. The sources used are trimethylgallium (TMGa), trimethylaluminium (TMAl), trimethylindium (TMIn), arsine and phosphine. The growth temperature was kept at 700 °C to ensure high-quality material in the whole range from GaInP to AlInP. All layers are undoped.

The MOVPE system is equipped with a LayTec EpiRAS 200 sensor measuring in the wavelength range between 1.5 eV (826 nm) and 5 eV (248 nm) and a fibre-coupled LayTec EpiR-MF for the wavelength range from 0.75 eV (1653 nm) to 3.1 eV (400 nm). The EpiRAS is capable of measuring the reflectance anisotropy (RA) and the reflectance while the EpiR-MF is intended for reflectance measurements in a wide spectral range including also the IR. Since it is very difficult to measure the absolute reflectance in MOVPE under growth conditions we focused on the normalized reflectance $R/R_{ref}$, which is the actual reflectance of the growing layer stack divided by the reflectance reference given by the clean GaAs surface before growth was initiated ($R_{GaAs}$). The NR can furthermore be simulated by a multilayer growth model based on a high-temperature dielectric function database as it is implemented in LayTec's EpiSense software used for the RA and NR measurements. The composition of the $(Al_xGa_{1-x})_{1-y}In_yP$ layers were determined by photoluminescence, X-ray diffraction and electron microprobe.

## 3. Results and discussion

### 3.1. Composition dependence of reflectance anisotropy

At first, the dependence of the in situ measured RA signal on both $(Al_xGa_{1-x})_yIn_{1-y}P$ compositions $x$ (aluminium content) and $y$ (indium content) was studied. Fig. 1 shows the dependence of the RA signal on the aluminium content $x$ in $(Al_xGa_{1-x})_{0.52}In_{0.48}P$ for $x = 0$, 0.2, 0.5, 0.7, and 1. A clear change in the amplitude as well as in the energetic position of the main peak can be seen. The amplitude increases with increasing aluminium content and the energetic position of the main peak around 3 eV shifts to higher energies as the aluminium content increases. This composition dependence can be correlated to the aluminium dependence of the $E_1$ feature in the band structure [9].

For the evaluation of the dependence of the RA signal on the indium composition, the growth of three $(Al_{0.5}Ga_{0.5})_{1-y}In_yP$ layers with different indium content $y$ was followed by transient measurements at 3.5 eV (354 nm) for $y = 0.445$, 0.478, 0.510 as shown in Fig. 2. A strong dependence of the RA signal can also be seen. These measurements were also done for the ternary materials GaInP and AlInP. The RA signal difference $RA_{AlGaInP-RAGaAs}$ was then calculated and the results are summarized in Fig. 3 for five different aluminium compositions $x$ and three different values for the lattice mismatch (i.e. indium composition $y$), respectively. As can clearly be seen the RA signal difference represents both compositions $x$ and $y$ with an increasing sensitivity to the indium content with increasing aluminium composition. Knowing one of the compositions ($x$ or $y$) the other one can be estimated from this dependence.

However, the disadvantage of the RA measurement (which is usually its advantage) is the additional sensitivity of the RA signal to other layer and surface properties. This can be caused, e.g. by a different phosphorus coverage which results in a different surface reconstruction [10] or a different doping level [6]. Therefore an absolute composition determination should be based on a bulk related effect. In the following we therefore focus on the normalized reflectance.

### 3.2. Composition dependence of normalized reflectance

Fig. 4 shows NR transients taken at 3.5 eV during growth of a test structure consisting of three lattice

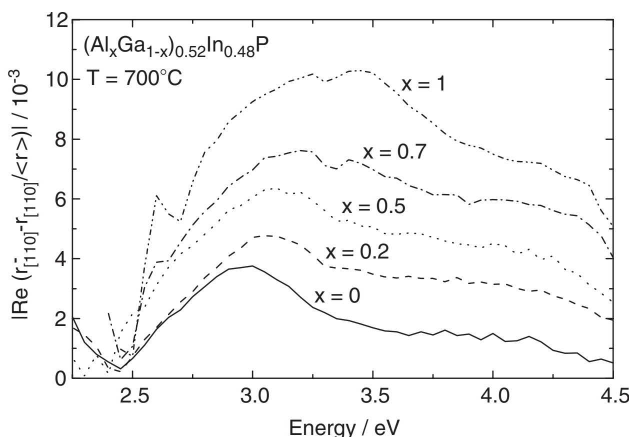


Fig. 1. Dependence of RA spectra on aluminium content $x$ in lattice-matched $(Al_xGa_{1-x})_{0.52}In_{0.48}P$ layers at 700 °C.

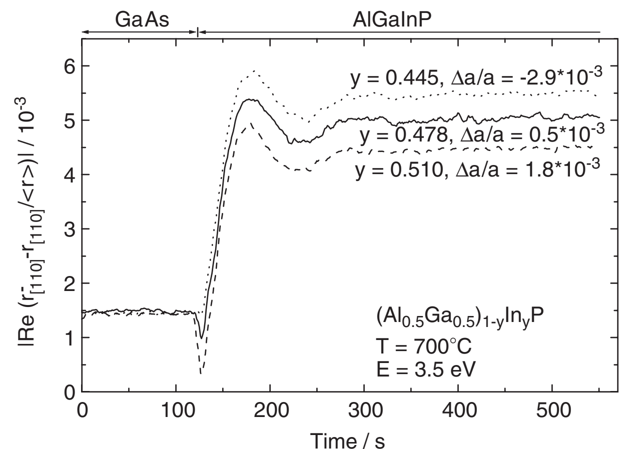


Fig. 2. RA transients taken at 3.5 eV during growth of three different $(Al_{0.5}Ga_{0.5})_{1-y}In_yP$ layers around the lattice-matched value of $y = 0.484$ at 700 °C.

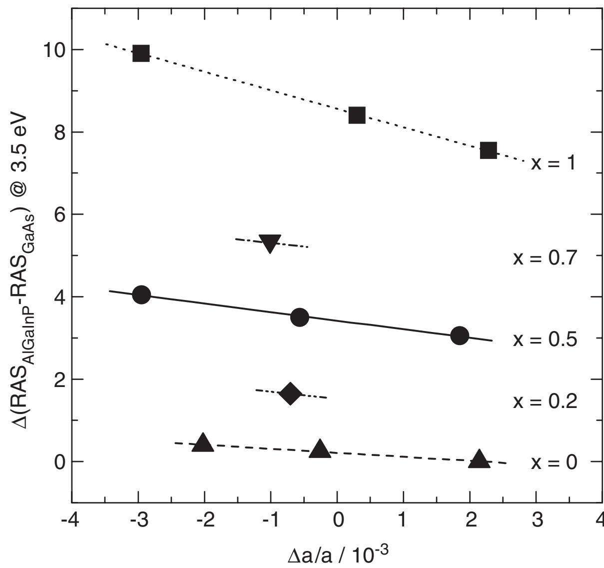


Fig. 3. Dependence of the RA signal ($RA_{AlGaInP}-RA_{GaAs}$) at 3.5 eV for different aluminium contents $x$ and lattice mismatch values (i.e. indium content $y$).

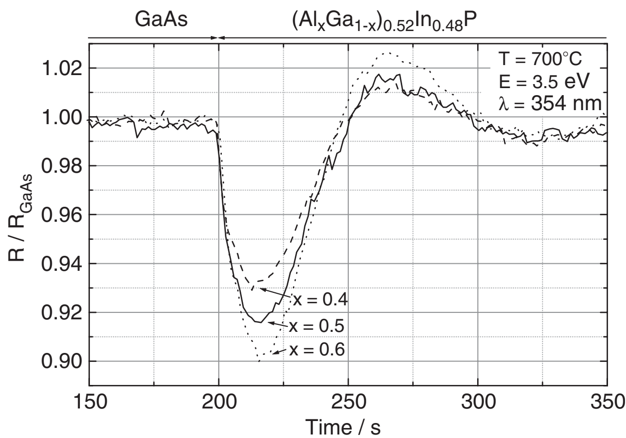


Fig. 4. NR transients taken at 3.5 eV during growth of a test structure including three different $(Al_xGa_{1-x})_{0.52}In_{0.48}P$ layers with aluminium content as indicated.

matched $(Al_xGa_{1-x})_{0.52}In_{0.48}P$ layers with aluminium contents of $x = 0.4$, 0.5, and 0.6. Starting from the GaAs level the transients show a significant dependence on the aluminium content in the $(Al_xGa_{1-x})_{0.52}In_{0.48}P$ layers when growth starts. In particular the amplitude of the first minimum of the Fabry–Perot interference directly correlates to the aluminium composition $x$. With increasing aluminium content the amplitude of the Fabry–Perot interference increases due to the higher difference of the optical constants between GaAs and $(Al_xGa_{1-x})_{0.52}In_{0.48}P$. Growth of very thin calibration layers is therefore sufficient.

Investigating the indium composition dependence, Fig. 5 shows NR transients taken also at 3.5 eV during growth of a test structure consisting of three differently strained only

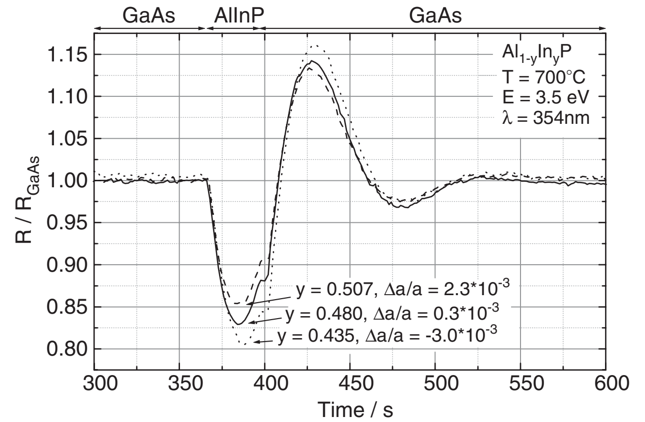


Fig. 5. NR transients taken at 3.5 eV during growth of a test structure including three differently strained very thin (12 nm) $Al_{1-y}In_yP$ layers.

12 nm thick $Al_{1-y}In_yP$ layers. Growth of the respective $Al_{1-y}In_yP$ layers was stopped after the first half of the Fabry–Perot interference to minimize the incorporated strain and suppress formation of defects. As it can be seen that the minimum amplitude clearly correlates to the indium content of the layer. The amplitude of the Fabry–Perot interference increases with decreasing indium content due to the increasing difference between the optical constants of GaAs and $(Al_xGa_{1-x})_{0.52}In_{0.48}P$ with reduced indium content.

With these reflectance transients it is therefore possible to calibrate the aluminium content $x$ or the indium content $y$ individually. Due to the high sensitivity of the signal this can even be done using very thin layers. However, the effect of the respective composition changes in $x$ and $y$ on the optical signal is similar in both cases. For in situ calibration procedures it must therefore be investigated how the two compositions $x$ and $y$ can be separated which will be discussed in the next paragraph.

### 3.3. Calibration procedures

The calibration of growth parameters for $(Al_xGa_{1-x})_{0.52}In_{0.48}P$ growth (e.g. after having done changes in the growth system or for transferring a growth process to a different reactor) is rather time consuming since a series of test samples and ex situ characterization measurements are needed. Therefore, an in situ calibration procedure which uses several thin calibration layers in only a few test samples would be very useful. Taking into account the results presented above the following two in situ calibration procedures for both compositions $x$ and $y$ can be proposed.

The first way is to start with the aluminium composition $x$. This value can be calibrated independently by growing $Al_xGa_{1-x}As$ layers as demonstrated earlier by Haberland et al. [11]. In this work it was found that the aluminium content $x$ in $Al_xGa_{1-x}As$ also has a strong impact on the amplitude of the first Fabry–Perot interference which

occurs during growth of $Al_xGa_{1-x}As$ layers on GaAs. Since the aluminium incorporation is the same for $Al_xGa_{1-x}As$ and $(Al_xGa_{1-x})_{0.52}In_{0.48}P$ the resulting aluminium composition can be transferred from the $Al_xGa_{1-x}As$ to the $(Al_xGa_{1-x})_{0.52}In_{0.48}P$ layers. This aluminium composition should then be used for the growth of $(Al_xGa_{1-x})_{0.52}In_{0.48}P$ with the desired $x$ value. The $y$ value can then be determined by reflectance measurements on test structures using $(Al_xGa_{1-x})_{1-y}In_yP$ layers with varying $y$. Due to the high sensitivity of the reflectance measurement these layers can be grown very thin giving the possibility to grow several of these layers in one single test structure.

For the second approach, we at first determined the growth rate of the respective $(Al_xGa_{1-x})_{0.52}In_{0.48}P$ layers. This was done in two different ways. Since the growth of the thick lattice matched $(Al_xGa_{1-x})_{0.52}In_{0.48}P$ layers was also followed by NR transient measurements at 2.2 eV (563 nm) the growth rate was determined by an optical fit to the measured Fabry–Perot interferences. For comparison the growth rate was also determined ex situ using thickness measurements by a scanning electron microscope (SEM). The results are summarized in Table 1. It can be seen that the difference between the growth rates determined in situ and ex situ is very small. The fits to the transients show only deviations in the range of 1% from the values determined by ex situ. From these results the growth efficiency (i.e. growth rate per partial pressure of the indicated sources) was calculated. The values displayed in Fig. 6 show the dependence on the aluminium content $x$ for different source combinations. For the sources TMAl + TMGa a decrease in growth efficiency with increasing aluminium content is found while it is slightly increasing for TMIn. For the sum of all three sources the growth efficiency remains constant over the whole range. Using the dependence of the growth efficiency on the aluminium content $x$ for TMAl + TMGa an in situ determination of the growth efficiency via the in situ fitted growth rate and the known partial pressures of the respective sources should enable the in situ determination on the aluminium content $x$. However, before doing this the indium content should be adjusted via the two ternary compounds $Ga_{1-y}In_yP$ and $Al_{1-y}In_yP$ by using the technique demonstrated in Fig. 5. For these two compounds no influence of the aluminium composition $x$ is obviously present and therefore an independent calibration of the indium composition $y$ is possible. In the following with the flow rates adjusted by in situ NR measurements and the growth efficiency characteristics of the reactor accurately measured any $(Al_xGa_{1-x})_{0.52}In_{0.48}P$ composition can be adjusted in situ. The measured growth rate is then used for double checking the composition via the growth efficiency.

Table 1
Growth rates for lattice-matched $(Al_xGa_{1-x})_{0.52}In_{0.48}P$ layers determined by fits of the optical data to the transients taken at 2.2 eV and from ex situ SEM measurements

| $x$ | Growth rate (ex situ, SEM) (nm/s) | Growth rate (in situ, 2.2 eV) (nm/s) | $\Delta$ (SEM, NR at 2.2 eV) (%) |
|---|---|---|---|
| 0 | 0.453 | 0.457 | 1.0 |
| 0.2 | 0.426 | 0.414 | −2.8 |
| 0.5 | 0.436 | 0.428 | −1.8 |
| 0.7 | 0.433 | 0.429 | −0.8 |
| 1 | 0.413 | 0.409 | −0.8 |

The last column shows their difference in percent.

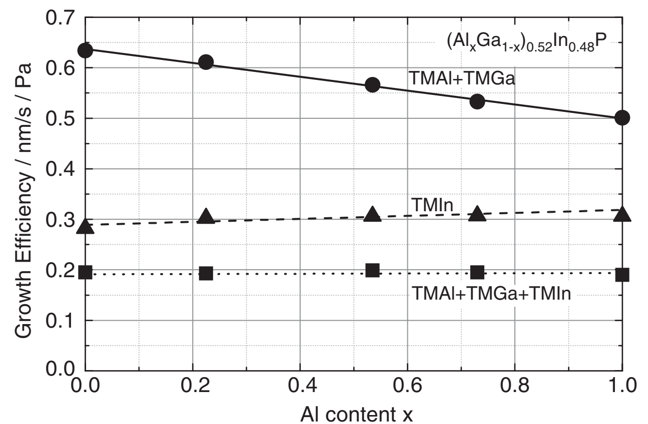


Fig. 6. Growth efficiency (growth rate per partial pressure of the indicated sources) for the growth of lattice-matched $(Al_xGa_{1-x})_{0.52}In_{0.48}P$.

## 4. Summary

We have investigated the dependence of the in situ measured reflectance (R) and reflectance anisotropy (RA) signal on the aluminium composition $x$ and the indium composition $y$ of $(Al_xGa_{1-x})_{1-y}In_yP$ layers. The results show a clear shift of the RA and R signal with both compositions. This can be seen in spectroscopic as well as in time-resolved measurements. In the time-resolved measurements the composition can be determined after growing about 12 nm thick layers by analysing the first minimum of the UV Fabry–Perot interference. This is advantageous because this minimizes the incorporated strain due to the lattice-matched composition.

Two procedures to establish an in situ composition calibration have been proposed. By analysing the growth efficiency via the in situ determined growth rate it is possible to separate the aluminium content $x$ from the indium content $y$.

## References

[1] K. Streubel, N. Linder, R. Wirth, A. Jäger, IEEE J. Sel. Top. Quant. Electron. 8 (2002) 321.
[2] D.P. Bour, R.S. Geels, D.W. Treat, T.L. Paoli, F. Ponce, R.L. Thronton, B.S. Krusor, R.D. Bringans, D.F. Welch, IEEE J. Quant. Electron. 30 (1994) 593.
[3] M. Zorn, A. Knigge, U. Zeimer, A. Klein, H. Kissel, M. Weyers, G. Tränkle, J. Crystal Growth 248 (2003) 186.

[4] D.E. Aspnes, Mater. Sci. Eng. B 30 (1995) 109.
[5] J.-T. Zettler, K. Haberland, M. Zorn, M. Pristovsek, W. Richter, P. Kurpas, M. Weyers, J. Crystal Growth 195 (1998) 151.
[6] M. Zorn, M. Weyers, J. Crystal Growth 276 (2005) 29.
[7] P. Wolfram, E. Steimetz, W. Ebert, N. Grote, J.-T. Zettler, J. Crystal Growth 272 (2004) 118.
[8] C. Watatani, Y. Hanamaki, M. Takemi, K. Ono, Y. Mihashi, T. Nishimura, J. Crystal Growth 281 (2005) 227.
[9] K. Haberland, A. Bhattacharya, M. Zorn, M. Weyers, J.-T. Zettler, W. Richter, J. Electron. Mater. 29 (2000) 468.
[10] M. Zorn, T. Trepk, J.-T. Zettler, B. Junno, C. Meyne, K. Knorr, T. Wethkamp, M. Klein, M. Miller, W. Richter, L. Samuelson, Appl. Phys. A 65 (1997) 333.
[11] K. Haberland, A. Kaluza, M. Zorn, M. Pristovsek, H. Hardtdegen, M. Weyers, J.-T. Zettler, W. Richter, J. Crystal Growth 240 (2002) 87.